Validation of an Outdoor Coast-Down Test to Measure Bicycle Resistance Parameters

Simone Tengattini[1] and Alexander Bigazzi, Ph.D.[2]

Abstract: Bicyclist rolling and aerodynamic resistance parameters are needed to estimate speed and energy expenditure in various travel analysis applications. These parameters have been investigated for sport and professional bicyclists, but better understanding is needed for real-world urban bicyclists. This paper describes a field coast-down test to measure bicycle resistance parameters that can be administered during traveler intercept surveys and generate representative data for advanced bicycle travel models. Mathematical models are developed that expand on past methods by accounting for varying wind and grade and allowing for increased measurement locations per test. A 12-sensor, 100-m test setup is developed, and indoor and outdoor validation tests are performed. The additional measurement locations yield higher precision than the previous three-sensor methods, but as expected, the precision of outdoor tests is lower due to inconsistent wind, grade, and riding surface. Outdoor validation tests generate rolling resistance coefficient estimates of 0.0064 ± 0.0013 and effective frontal area estimates of 0.63 ± 0.11 m^2. Outdoor tests in a headwind are sufficiently sensitive to identify significant changes in resistance with riding position and tire pressure and are expected to generate realistic parameter estimates for parsimonious modeling of on-road bicyclists.
DOI: 10.1061/JTEPBS.0000152.

Author keywords: Bicycles; Power; Aerodynamic drag; Rolling resistance.

Introduction

With the growth in bicycling as an urban transportation mode in cities around the world, there is increasing interest in, and need for, methods to model bicycle performance and bicyclist behavior in increasing detail. Bicycle performance, particularly design speed, is a key input for safe, reliable, and attractive infrastructure design (Navin 1994; Parkin and Rotheram 2010). Better understanding of bicycle speed and how it relates to energy expenditure could improve understanding of bicycle route and mode choices (Heinen et al. 2010; Iseki and Tingstrom 2014; Mercat 1999). Speed and energy expenditure are also important factors for health effects through air pollution and physical activity, and better characterization could improve health assessments for transportation systems and projects (Bigazzi 2017; Bigazzi and Figliozzi 2014; Mueller et al. 2015).

Bicyclist power and energy expenditure are connected to travel (speed) and roadway (grade and pavement) conditions primarily through inertial mass and physical parameters describing rolling and aerodynamic resistances (Bigazzi and Figliozzi 2015; Olds 2001; Wilson 2004). These parameters have been investigated, mainly for sport and professional bicycling, while relatively little is known about their values for utilitarian urban bicyclists (Bigazzi and Figliozzi 2015; Faria et al. 2005; Wilson 2004). Utilitarian bicyclists could have systematically different equipment and power levels from sport riders, and it is unlikely that sport-oriented data are representative of the broader population of urban bicyclists. A better understanding of the values of these physical parameters for real-world urban bicyclists is needed to accurately estimate speed and energy expenditure and advance representation of bicycles in transportation system analysis.

To measure resistance parameters for large representative samples of in-use bicycles, a practical intercept test method is needed that can be implemented in situ on bicycle facilities, imposes minimal burden on participants (ideally completed within a few minutes), and does not substantially alter the condition of the bicycle being tested. Aerodynamic drag and rolling resistances during bicycling have been investigated using various methods, including wind tunnels, power meters, field methods, and coast-down tests (Debraux et al. 2011; Kyle and Burke 1984; Martin et al. 1998; Wilson 2004). Wind tunnel testing is highly accurate, but measures only aerodynamic drag and cannot be implemented in situ. Field-based power-meter and virtual elevation methods are impractical for intercept testing because they require extended riding times and installation of a device that would likely deter participation, are not compatible with all bicycles, and could change the resistance characteristics of the tested bicycles.

Coast-down testing, also known as the deceleration method, is appealing for testing of intercepted bicyclists because it can capture both rolling and drag resistance forces, has been successfully applied to a range of vehicles, can be implemented in situ without modifying a participant's bicycle, and requires only a few minutes to complete. A coast-down test consists of measuring a vehicle's motion while coasting from a cruising speed to a stop without activating the brakes, and then extracting resistance parameters from the data by fitting a physical equation of motion (Candau et al. 1999; Debraux et al. 2011; Kyle and Burke 1984; Preda and Ciolan 2010; White and Korst 1972). While this method holds promise, most previous bicycle coast-down testing has been conducted indoors, and so the method must be revised for field application by accounting for wind and grade.

The objective of this paper is to develop and validate a field bicycle coast-down test that can be administered during traveler

[1]Masters Student, Dept. of Civil Engineering, Univ. of British Columbia, Vancouver, BC, Canada V6T 1Z4. Email: simone.tengattini@alumni.ubc.ca

[2]Assistant Professor, Dept. of Civil Engineering, Univ. of British Columbia, 2029-6250 Applied Science Lane, Vancouver, BC, Canada V6T 1Z4 (corresponding author). Email: abigazzi@civil.ubc.ca

Note. This manuscript was submitted on November 11, 2016; approved on January 5, 2018; published online on April 28, 2018. Discussion period open until September 28, 2018; separate discussions must be submitted for individual papers. This paper is part of the ***Journal of Transportation Engineering, Part A: Systems***, © ASCE, ISSN 2473-2907.

intercept surveys and generate data for advanced bicycle travel models. Mathematical models for indoor and outdoor coast-down conditions are presented in the next section, along with a description of the instrumentation and the validation test conditions. Indoor and outdoor test results are then presented, followed by a discussion of implications for implementation during intercept surveys and future work. Limitations of the approach are also discussed.

Method

Previous Coast-Down Tests

In the absence of propulsion or braking forces, vehicle deceleration is primarily determined by rolling, aerodynamic, and grade resistance forces. For automobiles, the coast-down test is formalized as a velocity–time curve from the basic equations of motion, and onboard instruments (e.g., accelerometers, tachometers, and odometers) can be used to measure instantaneous deceleration, speed, and distance over time (Preda and Ciolan 2010; White and Korst 1972). Coast-down deceleration on level ground can be represented as the differential equation

$$m \cdot \frac{dv}{dt} = c_0 + c_1 v + c_2 v^2 \tag{1}$$

where m = total mass of the vehicle; v = instantaneous speed over time t; and c_i = resistance parameters. Typically, rolling resistance is considered to be independent of speed (contributing to c_0) and drag proportional to v^2 (contributing to c_2); c_1 is usually low, related to the rotational speed, and sometimes assumed to be zero (di Prampero et al. 1979).

Onboard measurement is slightly more difficult for bicycles (for example, using power meters or cycle computers)—particularly during a short field test with intercepted travelers. Waltham and Copeland (1999) manually recorded velocity over time with an audio recorder, while de Groot et al. (1995) logged cycle computer data and used Eq. (1) with $c_1 = 0$ to develop the fitting equation for $v(t)$

$$v = \sqrt{\frac{c_0}{k_m}} \tan\left(\operatorname{atan}\left(v_0\sqrt{\frac{k_m}{c_0}}\right) - \sqrt{c_0 k_m}\, t\right) \tag{2}$$

where v_0 = initial bicycle speed; and k_m = aerodynamic drag per unit mass (c_2/m). Cycle computers to measure speed are problematic for a field survey because each bicycle would have to be instrumented before testing. In addition, there are resolution errors at low speeds for most off-the-shelf cycle computers.

As an alternative to direct speed measurements, time measurement at fixed locations has been used for bicycle coast-down test instrumentation. Kyle and Burke (1984) performed coast-down tests with bicyclists coasting down a hill then slowing to a stop on flat land. Initial coasting speed was measured using time traps (two timing switches a short distance apart) and the total coasted distance was recorded. The equation developed for the test coasting distance was

$$x = \frac{m}{2c_2}\ln\left(\frac{-mgG + c_0 + c_2(v_0 - w)^2}{-mgG + c_0 + c_2 w^2}\right) + \frac{mw}{\sqrt{c_2(-mgG + c_0)}}\left(-\operatorname{atan}\left(\frac{-w\sqrt{c_2}}{\sqrt{-mgG + c_0}}\right) + \operatorname{atan}\left(\frac{c_0 - mgG + c_2 v_0^2}{-mgG + c_0}\right)\right) \tag{3}$$

where m = mass of rider and bicycle; c_0 and c_2 = rolling and drag resistance parameters; g = gravitational acceleration; G = road grade; and w = wind speed. Results of the on-road testing were inconclusive, possibly due to lack of accounting for varying wind and grade.

Candau et al. (1999) developed an indoor coast-down test using three timing switches (pneumatic tubes) in a flat hallway, with spacing of 1 and 20 m. Trigger times were recorded using a computer chronometer with resolution of 30 μs. They developed a mathematical framework from Eq. (1) with $c_1 = 0$, similar to Eq. (3) but without grade and wind effects. A first estimate of v_0 was obtained from the first two timing sensors with spacing of x_0 and initial time t_0, and then the timing for the third switch estimated by

$$x(t) = \frac{m}{2c_2}\ln\left[\frac{1 + \tan\left(t\sqrt{c_0 c_2/m^2} - \operatorname{atan}\left(\frac{\cos(t_0\sqrt{c_0 c_2/m^2}) - e^{\frac{c_2}{m}x_0}}{\sin(t_0\sqrt{c_0 c_2/m^2})}\right)\right)^2}{1 + \frac{c_2}{c_0}\left(\sqrt{\frac{c_0}{c_2}}\cdot\frac{\cos(t_0\sqrt{c_0 c_2/m^2}) - e^{\frac{c_2}{m}x_0}}{\sin(t_0\sqrt{c_0 c_2/m^2})}\right)^2}\right] \tag{4}$$

Parameter estimates for c_0 and c_2 were generated by minimizing the squared difference between $x(t)$ from Eq. (4) and the measured distance of 20 m.

Mathematical Formulation

Our field bicycle coast-down test builds on this past work by introducing dynamic wind and grade variables as well as multiple timing measurements over a longer coasting distance. The motivation for the additional measurements is to try to compensate for the noise expected to be introduced by varying on-road conditions (grade, wind, and pavement) as well as to allow parameter estimation from a single test of an intercepted traveler (most previous coast-down testing involved dozens of runs for a single bicycle/rider, which would be a major burden for field intercept surveys). In addition, because the data are collected as $t(x)$, new expressions are derived that provide residuals in the measurement dimension [as opposed to $x(t)$].

Following previous coast-down studies, for an indoor test without wind or grade effects, rolling resistance force R_r is assumed to be independent of speed, and drag resistance force R_d is assumed to be proportional to the square of speed (Candau et al. 1999; de Groot et al. 1995; Kyle and Burke 1984; Waltham and Copeland 1999; Wilson 2004):

$$R_r = C_r mg \tag{5}$$

$$R_d = \frac{1}{2}\rho A_f C_d v^2 \tag{6}$$

where C_r = unitless rolling coefficient; m = mass of bicycle and rider in kg; g = gravitational acceleration in m/s^2; ρ = air density in kg/m^3; A_f = frontal area in m^2; C_d = unitless drag coefficient; and v = speed in m/s. Note that wind and grade may also affect indoor tests but were not accounted for in previous estimation methods. The product $A_f C_d$ is known as effective frontal area. Air density is a function of altitude (proxy for barometric pressure) and temperature (di Prampero 1986)

$$\rho = \rho_0 \cdot e^{-0.127h} \cdot \left(\frac{273}{T}\right) \tag{7}$$

where $\rho_0 = 1.293$ kg/m^3; h = altitude above sea level (km); and T = absolute temperature (°K).

Similar to Eq. (1), coast-down resistance forces and deceleration can be formalized

$$m\frac{dv}{dt} = -R_r - R_d = -C_r mg - \frac{1}{2}\rho A_f C_d v^2 \tag{8}$$

Using the simplifying parameters $A = gC_r$ and $B = (1/2m)\rho A_f C_d$, Eq. (8) becomes the differential equation

$$\frac{dv}{dt} = -A - Bv^2 \tag{9}$$

Integration is performed by separating variables and enforcing boundary conditions $v(t_0) = v_0$, leading to

$$v(t) = \frac{v_0 - \sqrt{\frac{A}{B}}\tan(t\sqrt{AB})}{v_0\sqrt{\frac{B}{A}}\tan(t\sqrt{AB}) + 1} \tag{10}$$

Then, using $v(dv/dx) = dv/dt$ and Eq. (9), and integrating with the boundary condition $x(v_0) = 0$

$$x(v) = \frac{1}{2B}\ln\left(\frac{A + Bv_0^2}{A + Bv^2}\right) \tag{11}$$

Finally, substituting Eq. (10) in Eq. (11) and rearranging

$$t(x) = \frac{1}{\sqrt{AB}}\text{atan}\left(\frac{\sqrt{AB}v_0 - \sqrt{A^2e^{2Bx} - A^2e^{4Bx} + ABv_0{}^2e^{2Bx}}}{Ae^{2Bx} - Bv_0^2}\right) \tag{12}$$

which is the indoor coast-down equation for multiple sensor locations (without wind and grade effects).

Velocity vectors for outdoor test conditions are illustrated in Fig. 1, where absolute wind speed w_{abs} and direction α are measured by an anemometer. The apparent wind vector $\overrightarrow{w_{app}}$ is the vector difference between measured wind $\overrightarrow{w_{abs}}$ and bicycle ground speed $\vec{v}$; β is the yaw angle. For outdoor testing with varying wind and grade over x, Eq. (6) is revised to

$$R_d = \frac{1}{2}\rho A_f C_d(w_{app}\cdot\cos(\beta - \pi))|w_{app}\cdot\cos(\beta - \pi)| \tag{13}$$

Eq. (13) can be rewritten $R_d = 1/2\rho A_f C_d(v - w)|v - w|$, where w is wind speed (w_{abs}) in the direction of travel. The absolute value in Eq. (13) ensures that the drag force acts in the correct direction when a tailwind exceeds the travel speed, i.e., $v - w < 0$ (Knight 2008).

This simplified formulation of drag resistance employs a single bicycle parameter, the effective frontal area, consistent with most previous methods (Candau et al. 1999; de Groot et al. 1995; Kyle and Burke 1984; Waltham and Copeland 1999; Wilson 2004). A more comprehensive representation of aerodynamic forces would include effective area and wind in three dimensions creating front, side, and lift forces and moments (Fintelman et al. 2014; Isvan 2015). Other previous work modeling on-road power employed a similar single-parameter formulation, but varied the effective frontal area with yaw angle, based on wind tunnel testing (Martin et al. 1998). The single parameter method is a limitation but was selected as the preferred approach because (1) it does not require testing in varying wind conditions, which would be impractical in an intercept survey; and (2) it generates a parsimonious set of two resistance parameters, which can be readily implemented in travel modeling applications. Three-dimensional wind vectors and resistance parameters can be more precise, but the simplified approach is likely closer to what will ultimately be used in travel models. Limitations are further discussed subsequently.

Grade resistance is $R_g = mgG/sqrt(1 + G^2)$, which for small grades can be simplified to

$$R_g = mgG \tag{14}$$

Eq. (8) is then revised to

$$m\frac{dv}{dt} = -R_r - R_g - R_d = -mg(C_r + G) - \frac{1}{2}\rho A_f C_d(v - w)|v - w| \tag{15}$$

Eq. (9) becomes the differential equation

$$\frac{dv}{dt} = -A - gG - B(v - w)|v - w| \tag{16}$$

which can be inverted to

$$\frac{d^2t}{dx^2} = \left(\frac{dt}{dx}\right)^3\left[A + gG + B\left(\left(\left(\frac{dt}{dx}\right)^{-1} - w\right)\cdot\left|\left(\frac{dt}{dx}\right)^{-1} - w\right|\right)\right] \tag{17}$$

For outdoor conditions, G, v, and w all vary over t and x. Due to the time dependence of these variables and the presence of an absolute value function, no known indefinite integral exists to

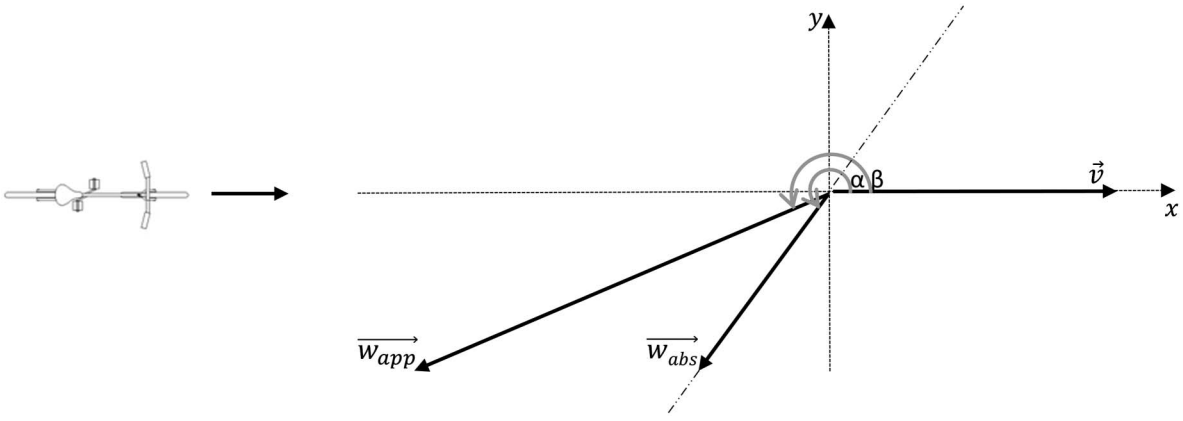

Fig. 1. Illustration of speed vectors and angles.

J. Transp. Eng., Part A: Systems, 2018, 144(7): 04018031

generate an analytical solution to Eq. (16). Therefore, a numerical, finite-element method is used to generate $t(x)$ using Eq. (17), starting from the boundary condition $t_0 = 0$, $x_0 = 0$, and $(dt/dx)_0 = (1/v_0)$, along with measured data for G and w. Wind at location x was assessed as $w(t(x))$.

Eqs. (12) and (17) provide methods for generating $t(x)$ from the parameters A, B, and v_0. Parameter estimates $\hat{A}$, $\hat{B}$, and $\hat{v}_0$ are generated by minimizing the sum of square error between the predicted times $t(x)$ and observed times $\tau(x)$ at each measurement location x_i

$$\sum_i [\tau(x_i) - t(x_i)]^2 \tag{18}$$

Eqs. (12) and (17) are both highly nonlinear, and the solution space contains many local minima. Parameter estimates are generated using a genetic algorithm for floating-point values with local nonlinear search optimization implemented in the statistical software R with the package GA (Scrucca 2013). Bounds for A and B were set using measured m, $g = 9.81$ m/s^2, ρ according to Eq. (7), a C_r range of 0.001–0.02, and a $A_f C_d$ range of 0.2–1.2 m^2, based on the literature, especially Wilson (2004). Bounds for v_0 were set at 3–6 m/s, based on field observations. The step size for the finite-element method was set at 1 m to facilitate reasonable processing time; shorter step sizes were explored for individual tests and were found to have no major impact on parameter estimates. The fitness function to maximize was the negative of Eq. (18). Additional algorithm parameters were selected based on initial fitting trials: population size 50, maximum iterations 2,000, termination at 150 iterations without improved maximum fitness, mutation probability 10%, and crossover probability 80%. As an alternative parameter fit for the simpler Eq. (12) method, Eq. (18) was minimized using a global nonlinear optimization search in MatLab (local solver lsqcurvefit run from multiple starting points using MultiStart).

Instrumentation

Fig. 2 provides an illustration of the test setup and instrumentation. The paired sensors at the start of the test were used to make a comparison with the method in Eq. (4) (Candau et al. 1999). Infrared break-beam sensors were used as timing switches. The 15° default beam angle was reduced using washers on both the emitter and the receiver. Response time and cross-interference of the sensors was tested during piloting and was found to be sufficient for detecting a 4-cm diameter rod (approximatively the width of a bicycle tire) at 6.5 m/s. Beam-break times were recorded by a microcontroller (Arduino Mega 2560) reading at ≤17 μs intervals and logging on a microSD card.

Wind speed and direction were measured using an ultrasonic anemometer (Young Ultrasonic 2D Anemometer, model 85000) placed at the start of the deceleration zone and connected to the microcontroller. Wind data were logged at 1 Hz, and the disaggregate second-by-second data were used in the coast-down equation [w in Eq. (17)]. Grade was measured every 10 m using an optical level (Leica Jogger 24) and a stadia rod, with a resolution of <0.01%. Break-beam sensors were aligned and positioned using a 100-m measuring tape and a five-point self-leveling laser. All beam heights were set at 0.31 m. For comparison to the 12-switch method, the bicycle was equipped with a cycle computer (Garmin Edge 500) recording distance and speed at 1 Hz (based on wheel revolutions).

Validation Tests

Validation testing was performed in three sessions. The first session was indoors to quantify test performance in a controlled environment (i.e., without wind and grade) and compare instrumentations (three-switch or 12-switch method, cycle computer). The second and third sessions were performed outdoors on relatively flat terrain in two different wind scenarios (crosswinds/tailwind and headwind) and on two different surfaces. In all tests, the rider was instructed to pedal backwards to mimic real-world riding conditions.

Indoor tests were performed on May 29, 2016, in a flat hallway with smooth concrete at the University of British Columbia. The hallway length limited the test setup to 90 m. Hallway altitude of 81 m and indoor temperature of approximately 20°C yielded air density of $\rho = 1.192$ kg/m^3. An early-model Centurion Le-Mans road bicycle (approximately 30 years old) was used for the test, equipped with 3-cm commuter tires and two rear panniers. The rider was a 22-year-old male (78.1 kg, 183 cm). The mass of the rider and bicycle was 94.5 kg. Six different tests were performed, with 10–30 runs (coast-downs) each. The tests for all sessions are summarized in Table 1. The rider on the test bicycle in the test hallway is shown in Fig. 3.

Outdoor tests were performed in two different sessions, the first (Session A) on a running track and the second (Session B) on an asphalt-paved bikeway. Session B was designed to most closely represent typical riding conditions, on a real bikeway surface and with a dominant headwind. Session A represents less ideal test conditions, with a dominant tailwind and high-resistance riding surface. The track was selected because it is a consistent riding surface; testing on a wider variety of surfaces, such as gravel paths, is left for future work.

Tests in Session A were performed on June 24, 2016, at Memorial South Park in Vancouver, British Columbia. The weather was cloudy, 18°C, with 75% relative humidity and track altitude of 98 m, leading to air density $\rho = 1.197$ kg/m^2. The track surface was a dry polyurethane, notably more rough and soft than the indoor test surface. The same rider, with same clothing and bicycle from the indoor test were used (Fig. 4). At the time of the test, the weight of the rider and bicycle was 95.1 kg. Grade was slightly negative in the first half of the test (minimum of −0.1%) and slightly positive in the second half of the test (maximum of 0.6%).

Tests in Session B were performed on August 16, 2016, on the North Arm Trail bikeway in Vancouver, British Columbia.

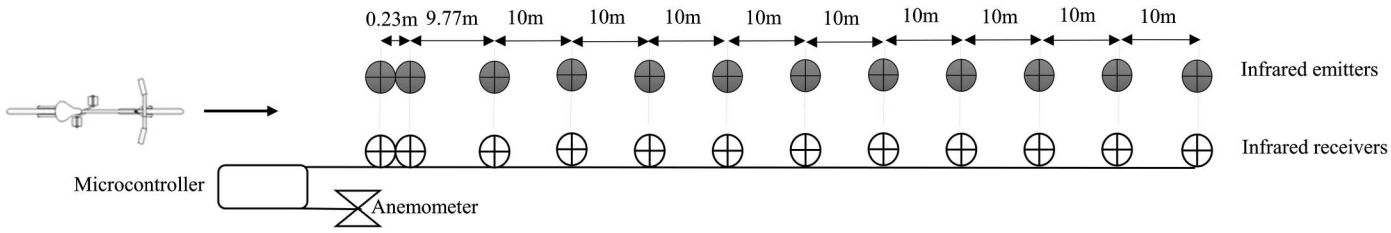

Fig. 2. Illustration of coast-down test setup.

J. Transp. Eng., Part A: Systems, 2018, 144(7): 04018031

Table 1. Test protocols for indoor and outdoor sessions

Test	Number of runs	Tire pressure (psi)	Riding position	Target v_0 (m/s)	Other
Baseline	30	80	Tops	4	—
Mass	10	80	Tops	4	10 kg added to panniers
Tire pressure	10	40	Tops	4	—
Riding position	10	80	Drops	4	—
Low speed	10	80	Tops	3	—
High speed	10	80	Tops	5	—

The weather was sunny, 23°C, with 68% relative humidity and at an altitude of 41 m, leading to air density $\rho = 1.186$ kg/m^3. The same rider with similar clothing and a similar bicycle from indoor testing and outdoor testing Session A were used (Fig. 4) (due to a crash, the LeMans was replaced with a Nishiki Rally road bicycle of similar age and condition, with 3-cm commuter tires and two rear panniers). At the time of the test, the mass of the rider and bicycle was 91.6 kg. Grade was slightly negative in most of the test (minimum of −0.8%) and slightly positive at the end (maximum of 0.4%).

Results

Indoor Test Results

Parameter estimation results for the indoor tests are given in Table 2. The results in the column "12-switch method" use the data from the infrared sensors illustrated in Fig. 2, the next column "Cycle computer data" uses the Garmin data as a comparison. Both columns were generated using Eq. (12). The last column, "three-switch method," applies Eq. (4) to the timing switch data as a comparison with Candau et al. (1999). Only the first 70 m of sensors were used for most of the indoor tests.

Parameter estimates are similar across the three methods in Table 2. Initial speed estimates are consistent with test protocols, and C_r and $A_f C_d$ values are in the range of literature values (Wilson 2004). The 12-switch method provides the best results in terms of reproducibility, i.e., the lowest standard deviations. In addition, sensitivity analyses revealed that standard deviations decrease with test length and increase with sensor spacing.

Parameter estimates are compared across tests for the 12-switch method data using two-tailed t-tests with a significance threshold of $p < 0.05$. The test results reveal significantly higher rolling resistance due to tire deflation ($p < 0.001$ for tire pressure versus baseline tests) and significantly lower effective frontal area due to riding in a drop position ($p = 0.02$ for riding position versus baseline tests). Parameter estimates were not significantly affected by mass, which is expected ($p = 0.87$ and $p = 0.27$ for C_r and $A_f C_d$, respectively, for mass versus baseline tests). However, the C_r estimates were significantly affected by initial speed ($p < 0.001$ for low speed versus baseline tests and $p = 0.03$ for high speed versus baseline tests), which could reflect a slight increase in C_r with speed, as suggested in some previous studies (Wilson 2004). Moreover, $A_f C_d$ estimates were unexpectedly affected by tire deflation ($p < 0.001$ for tire pressure versus baseline tests), which could also be due to a nonlinear positive speed dependence of C_r. Coast-down tests measure zero-order and second-order effects of speed on resistance, but do not otherwise differentiate rolling from aerodynamic resistance forces. Applying a nonparametric Mann-Whitney test instead of a t-test produces slightly different p-values, but does not change the hypothesis test results using a $p < 0.05$ threshold.

As a parameter-fitting diagnostic, the time residuals were compared across tests and sensor locations. The time residual at location i in test j is computed $\varepsilon_{i,j} = \tau(x_i) - t(x_i)$ [Eq. (18)]. The correlation of residuals by location [Fig. 5(a)] suggested small ~1-cm errors in the location data (i.e., sensor placement). For example, consistently positive residuals at one sensor location of around 0.005 s where the test bicycles are travelling at 1 m/s would indicate that the sensor location is off by approximately 0.005 m.

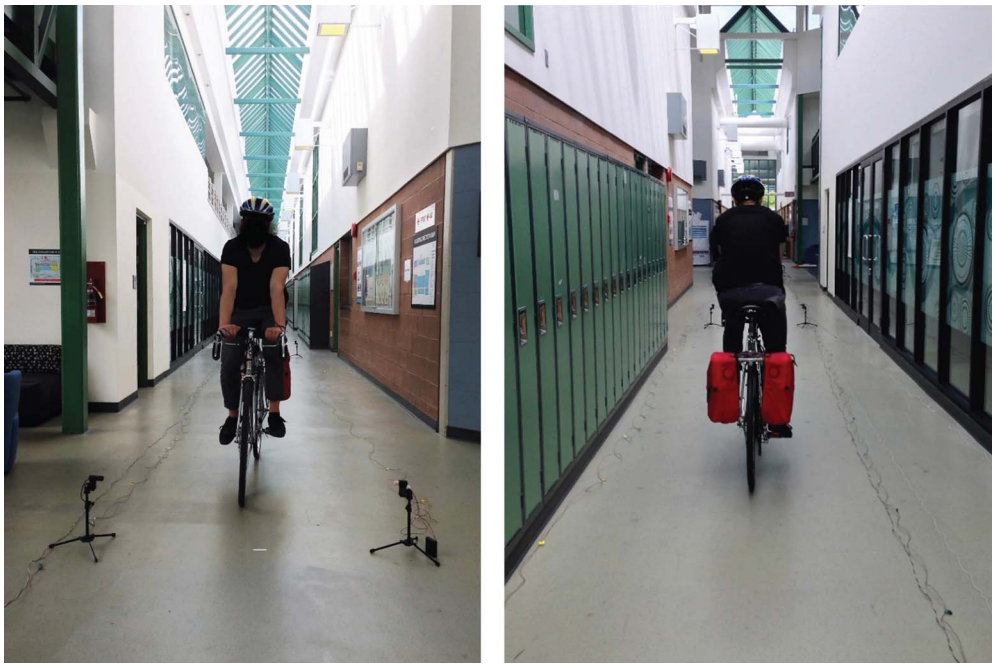

Fig. 3. Indoor test rider and bicycle coasting in tops position.

(a)

(b)

Fig. 4. Test rider coasting in tops position: (a) outdoor Session A; and (b) outdoor Session B.

Table 2. Indoor test parameter estimates: mean (standard deviation)

	12-switch method			Cycle computer data			Three-switch method		
Test	C_r	$A_f C_d$ (m^2)	v_0 (m/s)	C_r	$A_f C_d$ (m^2)	v_0 (m/s)	C_r	$A_f C_d$ (m^2)	v_0 (m/s)
Baseline	0.0051	0.449	3.99	0.0053	0.407	3.98	0.0062	0.502	4.17
	(0.0001)	(0.0285)	(0.10)	(0.0015)	(0.200)	(0.17)	(0.0003)	(0.0383)	(0.10)
Mass	0.0051	0.465	3.86	0.0047	0.436	3.73	0.0058	0.546	3.99
	(0.0002)	(0.0397)	(0.14)	(0.0015)	(0.216)	(0.14)	(0.0005)	(0.0675)	(0.12)
Tire pressure	**0.0066**	**0.560**	3.79	0.0057	0.6217	3.68	0.0073	0.604	3.94
	(0.0001)	(0.0344)	(0.08)	(0.0015)	(0.146)	(0.06)	(0.0004)	(0.0716)	(0.09)
Riding position	0.0052	**0.401**	3.94	0.0055	0.333	3.82	0.0057	0.475	4.06
	(0.0003)	(0.0497)	(0.08)	(0.0003)	(0.0413)	(0.08)	(0.0010)	(0.120)	(0.08)
Low speed	**0.0046**	0.415	2.77	0.0036	0.712	2.75	0.0053	0.596	2.94
	(0.0002)	(0.0698)	(0.08)	(0.0005)	(0.1250)	(0.08)	(0.0004)	(0.118)	(0.08)
High speed	**0.0054**	0.473	4.90	0.0062	0.375	4.70	0.0078	0.402	5.04
	(0.0003)	(0.0406)	(0.10)	(0.0013)	(0.131)	(0.13)	(0.0012)	(0.103)	(0.12)

Note: Bold values significantly different from baseline (two-tailed t-test with $p < 0.05$).

A location correction was performed on the timing switch data by adjusting the sensor locations (x_i) by $\Delta x_i = \overline{v_{i,j}\varepsilon_{i,j}}$, where $v_{i,j}$ and $\varepsilon_{i,j}$ are the speed and time residual at location i in test j. Location corrections (Δx_i) had a mean absolute value of 9 mm and a maximum of 26 mm. Time residuals from the parameter fits before and after location correction are shown in Fig. 5. The residual dispersion improved, but the parameter estimates were almost unchanged (<0.2% differences in C_r, $A_f C_d$, and v_0 estimates). The location correction was not applied to subsequent tests due to the negligible effect on parameter estimates; a lack of correlation in outdoor test residuals, and the doubling of the computational cost of fitting parameters with the correction (fitting already requires a day of processing time per session on a desktop computer).

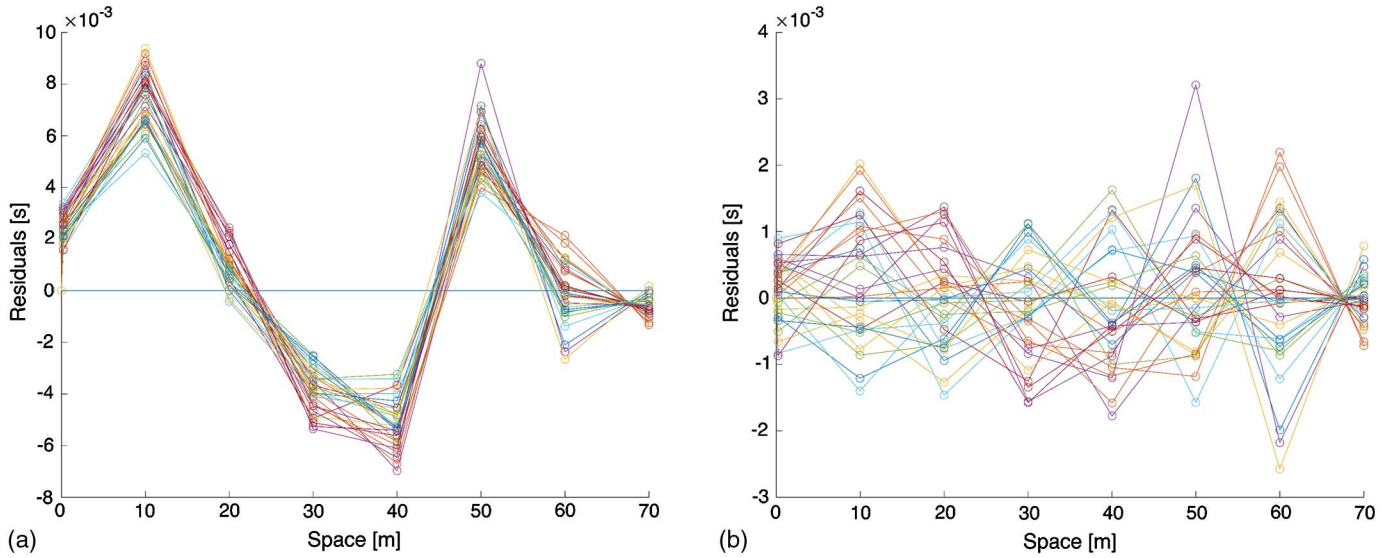

Fig. 5. Time residuals: (a) before; and (b) after location correction.

Outdoor Test Results

Parameter estimation results for the outdoor tests are given in Table 3 (only the 12-switch method was used for the outdoor tests). The parameter estimates in Table 3 have increased variability compared to the indoor tests, which is expected due to the influence of varying wind and grade. The outdoor timing switch standard deviations are comparable to those of the cycle computer and three-switch methods for the indoor tests. The initial speed estimates are again consistent with test protocols and cycle computer data, though the variation is higher than the indoor tests. Both the rolling resistance and effective frontal area parameters are higher than the indoor test results, but are still in the range of previously reported values (Wilson 2004). Road cyclist resistances are typically reported in the ranges of 0.002–0.010 for C_r and 0.2–0.6 m^2 for A_fC_d (Candau et al. 1999; Gross et al. 1983; Martin et al. 1998; Wilson 2004). The parameter estimates are consistent with expectations for a less sport-oriented upright cyclist with casual clothing and panniers (Figs. 3 and 4), which would have relatively high effective frontal area.

Table 3. Outdoor test parameter estimates: mean (standard deviation)

	Outdoor Session A			Outdoor Session B		
Test	C_r	A_fC_d (m^2)	v_0 (m/s)	C_r	A_fC_d (m^2)	v_0 (m/s)
Baseline	0.0102	0.692	4.25	0.0064	0.630	3.91
	(0.0011)	(0.111)	(0.12)	(0.0013)	(0.114)	(0.19)
Mass	**0.0116**	0.654	4.28	0.0061	0.567	4.03
	(0.0008)	(0.0815)	(0.08)	(0.0011)	(0.0984)	(0.14)
Tire pressure	0.0098	**0.793**	4.24	**0.0084**	0.594	3.87
	(0.0011)	(0.0839)	(0.11)	(0.0016)	(0.109)	(0.11)
Riding position	0.0108	0.670	4.29	0.0063	**0.539**	3.96
	(0.0007)	(0.152)	(0.13)	(0.0008)	(0.0638)	(0.16)
Low speed	0.0099	0.736	3.37	0.0057	0.623	2.99
	(0.0006)	(0.0638)	(0.13)	(0.0012)	(0.163)	(0.16)
High speed	0.0107	0.676	4.90	0.0062	0.640	4.71
	(0.0012)	(0.0726)	(0.14)	(0.0014)	(0.105)	(0.19)

Note: Bold values significantly different from baseline (two-tailed t-test with $p < 0.05$).

Higher outdoor than indoor C_r estimates can be expected from the rougher and softer surface on the running track in Session A and the rougher asphalt-paved surface in Session B. Higher outdoor A_fC_d estimates are likely due to the influence of real-world wind conditions as compared to the relatively still-air hallway. Previous wind tunnel tests and computational fluid dynamics simulations showed that crosswinds can increase effective frontal area due to increased frontal exposure (Fintelman et al. 2015, 2014). In addition, because the drag force is nonlinear with respect to relative air speed $v - w$, wind speed and direction variability (within the 1 s sampling frequency) would increase R_d and A_fC_d. Drag coefficient C_d generally varies with Reynolds number, particularly when apparent wind speed is below 10 m/s (Debraux et al. 2011; Defraeye et al. 2011), which could also lead to higher R_d and A_fC_d in outdoor wind conditions. Crosswinds can also lead to small movements by the bicyclist to adjust for varying lateral drag force (Fintelman et al. 2014), which could increase deceleration and estimated A_fC_d.

To illustrate the wind direction differences between tests, Fig. 6 shows the distribution of apparent wind speed and direction during the two outdoor sessions, separated into high (>3 m/s), medium (1.5–3 m/s), and low (<1.5 m/s) bicycle speed (v) ranges. Due to a dominant absolute crosswind/tailwind direction (α) during Session A, as bicycle coasting speed decreased the apparent wind direction (β) shifted away from a headwind. In contrast, Session B had a dominant headwind direction (α), which led to a more stable yaw angle (β) around 180°. The influence of crosswind on effective frontal area is supported by higher A_fC_d estimates with greater yaw angle (crosswind) in Session A than in Session B. The still-air hallway had essentially no crosswind, and the lowest A_fC_d estimates. Modified mathematical formulations were explored to include a dependence of A_fC_d on yaw angle based on published wind tunnel test results (Fintelman et al. 2014; Martin et al. 1998), but the parameter fits did not significantly improve. Future research should examine additional methods to account for wide yaw angles at low speeds and enable effective coast-down testing in a wider range of wind conditions.

Outdoor parameter estimates are again compared across tests using two-tailed t-tests with a significance threshold of $p < 0.05$. Parameter comparisons for Session B are all in line with expectations. Rolling resistance was significantly higher after tire

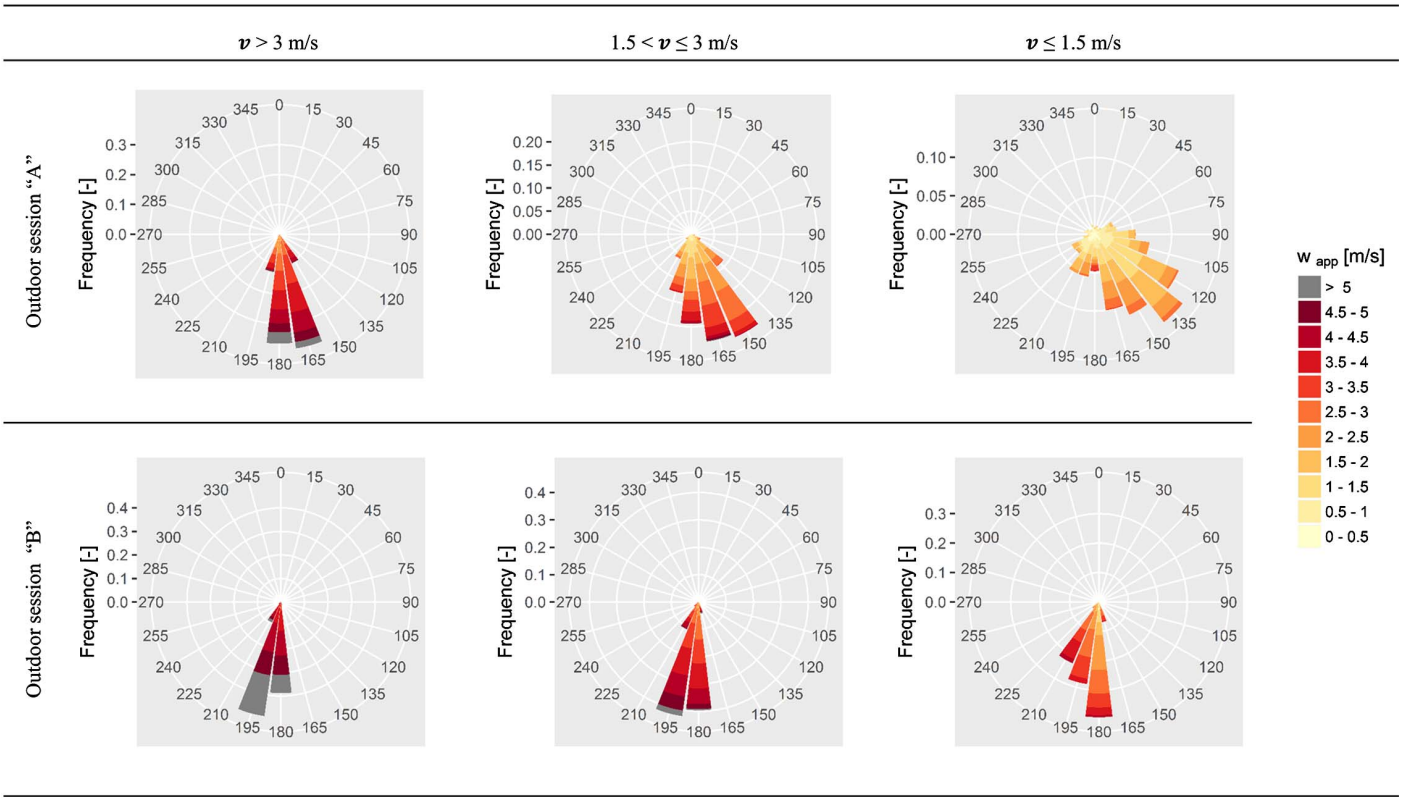

Fig. 6. Apparent wind speed and direction (β) for three bicycle speed intervals in outdoor test sessions.

deflation ($p < 0.001$ for tire pressure versus baseline tests), effective frontal area was significantly lower riding in a drop position ($p = 0.03$ for riding position versus baseline tests), and parameter estimates were not significantly affected by mass ($p = 0.58$, $p = 0.14$ for C_r and $A_f C_d$, respectively in test mass versus baseline) or initial speed ($p = 0.16$ and $p = 0.89$ for C_r and $A_f C_d$, respectively, for low speed versus baseline tests, and $p = 0.72$ and $p = 0.81$ for C_r and $A_f C_d$, respectively in high speed versus baseline tests). In contrast, Session A generated the unexpected results that rolling resistance was significantly higher with added weight ($p = 0.03$ for mass versus baseline tests) and effective frontal area was significantly higher after tire deflation ($p = 0.01$ for tire pressure versus baseline tests). The unexpected Session A results are possibly due to the very soft riding surface, on which C_r could vary with mass and speed (as discussed with the indoor test results). Another consequence of the softer riding surface was shorter total coasting distances for Session A (typically between 60 and 70 m) than for Session B (consistently the full 100 m), which generated fewer observations per test.

Conclusions

This paper presents a novel field coast-down test method to quickly measure physical resistance parameters for real-world urban bicyclists in situ. The test expands on previous methods by accounting for varying wind and grade and allowing for more measurement locations per test. The 12-sensor outdoor test achieves comparable precision to a three-sensor indoor test method, thus partially offsetting the effects of increased variability in outdoor conditions with increased observations per test.

Rolling resistance coefficient estimates were 0.0051 ± 0.0001, 0.064 ± 0.0013, and 0.0102 ± 0.0011 for tests on smooth concrete (indoors), asphalt pavement, and a polyurethane running track, respectively. Effective frontal area estimates were 0.45 ± 0.03 m^2, 0.63 ± 0.11 m^2, and 0.69 ± 0.11 m^2 for tests in still air (indoors), in a headwind, and in varying crosswind/tailwind, respectively. The parameter estimates are in line with expectations for utilitarian cyclists and confirm the importance of crosswind for aerodynamic drag resistance. The indoor test and the outdoor test on a hard surface with a dominant headwind were sufficiently sensitive to identify significant changes in resistance with tire pressure and riding position. The outdoor test in less ideal conditions (very soft riding surface and varying apparent wind direction) was not sufficiently sensitive to these changes, which is a limitation to consider for outdoor testing.

The two-parameter coast-down method directly measures the first-order and third-order effects of speed on resistance power. These two parameters are most representative of rolling and drag resistance coefficients, so they are presented in this paper as C_r and $A_f C_d$, as described in the "Method" section. However, the estimated values capture all first-order and third-order effects of speed. Lower-order drag effects can influence C_r and higher-order rolling effects can influence $A_f C_d$. Hence, they are specific to a two-parameter resistance model and should be applied and interpreted with caution outside of that framework. The results could equivalently be presented as the more abstract $A = gC_r$ and $B = 1/2$ m$(\rho A_f C_d)$ parameters—simple scalar transformations of the estimated physical parameters.

Ultimately, if the parameters will be used to estimate on-road bicyclist energy expenditure and speed, outdoor testing in a dominant headwind (e.g., Session B) is expected to generate the most representative values. Indoor $A_f C_d$ estimates will likely be too low due to approximately still-air test conditions and not representative of on-road cycling in varying wind. Parameter estimates from

outdoor tests with varying apparent wind direction (e.g., Session A) are less reliable and likely less representative of drag resistance at normal travel speeds.

The findings in this paper will be useful in experimental design and estimation of measurement error for implementing field coast-down tests in traveler intercept surveys. Parameter standard deviations of 0.001 for C_r and 0.1 for $A_f C_d$ should be sufficient to characterize the broad range of urban bicyclists. For example, samples of at least 20 observations would generate normal 95% confidence intervals of ± 0.0004 and ± 0.04 for C_r and $A_f C_d$, respectively—likely less than 10% of mean values. Tests are expected to yield better estimates if performed in headwind conditions with realistic yaw angles for normal travel speeds, and if the riders start with enough speed to coast the full 100 m.

Another possible application of the coast-down test is to generate field data of rolling resistance on different surface materials for bicycle facilities. A set of bicycles with representative tire types could be tested on various surfaces with consistent riders and wind conditions. Cycle computers could be used to generate test data with a simpler setup, but more test iterations would need to be performed due to the lower accuracy compared to the 12-switch instrumentation (Table 2).

For further validation, future work should compare measured power output on an instrumented bicycle with modeled power based on coast-down test results. In addition, outdoor test results can be compared with wind tunnel testing and other more precise methods of measuring bicycle resistance forces. Future work should also validate the test on a wider variety of riding surfaces and on varying road grades.

As stated previously, the simplified two-parameter representation of resistance forces is a limitation of the method. Modified field tests using additional aerodynamic and rolling resistance parameters could also be explored; for example, by adding second and third dimensions of effective area, explicit dependence of drag force on yaw angle, or speed dependence of rolling resistance. Estimating additional parameters from coast-down test data would likely increase parameter uncertainty.

More detailed approaches to modeling bicycle resistance forces with additional parameters have benefits and costs. The models can be more physically accurate and sensitive to factors such as rider shape and tire temperature, but they also require more data or assumptions to be applied. Parameter estimates for parsimonious approaches, such as those presented in this paper, can be generated from less invasive tests, enabling more representative samples in data collection. Hence, for modeling a large population of cyclists, there is a methodological trade-off between precision and representativeness, or measurement error versus sample error. The best approach depends on the ultimate objective and application. This study was designed with the goal of developing tools and data for analysts to use in transportation system analysis.

Currently, transportation system models do not explicitly incorporate bicycle power or energy, even emerging bicycle microsimulation models (Twaddle et al. 2014). In contrast, sports medicine has developed detailed, precise, and parameter-rich models of bicycle resistance forces and sport performance (Faria et al. 2005; Martin et al. 2007). The lack of representative data on utilitarian cyclists in the literature is indicative of either a lack of interest or a lack of measurement tools. There is a disconnect between the fields, and this work endeavors to bridge the gap with established methods simple enough to be integrated into transport system models. Given the current state of practice, we believe a model requiring many additional parameters for each cyclist would either be prohibitively complex or implemented with mostly default assumptions, negating the value of the added complexity. This research is a first step, and we hope the transport field moves in this direction, which will enable increasingly sophisticated models of cycling performance in practice.

Consider, as a parallel, the state of practice for motor vehicle fuel consumption and emissions models. Complex multiparameter models are used to simulate individual vehicles, such as Argonne National Laboratory's Autonomie. However, the primary model for project-level, regional, and national motor vehicle fuel and emissions estimates, the USEPA's Motor Vehicle Emissions Simulator (MOVES), uses just three parameters (besides mass) to characterize vehicle resistance forces—essentially the same coast-down parameters used in this paper (USEPA 2010).

Application of the field coast-down test in this paper is expected to generate new information about the physical characteristics of real-world bicyclists, which can be used to improve bicycle travel models and yield better understanding of on-road utilitarian bicycle performance.

Acknowledgments

This research was supported by the Natural Sciences and Engineering Research Council of Canada (NSERC) and the University of British Columbia. Andrei Radu assisted with the data collection.

References

Bigazzi, A. Y. 2017. "Determination of active travel speed for minimum air pollution inhalation." *Int. J. Sustainable Transp.* 11 (3): 221–229. https://doi.org/10.1080/15568318.2016.1238984.

Bigazzi, A. Y., and M. A. Figliozzi. 2014. "Review of urban bicyclists' intake and uptake of traffic-related air pollution." *Transp. Rev.* 34 (2): 221–245. https://doi.org/10.1080/01441647.2014.897772.

Bigazzi, A. Y., and M. A. Figliozzi. 2015. "Dynamic ventilation and power output of urban bicyclists." *Transp. Res. Rec.* 2520: 52–60. https://doi.org/10.3141/2520-07.

Candau, R. B., F. Grappe, M. Menard, B. Barbier, G. Y. Millet, M. D. Hoffman, A. R. Belli, and J. D. Rouillon. 1999. "Simplified deceleration method for assessment of resistive forces in cycling." *Med. Sci. Sports Exercise* 31 (10): 1441. https://doi.org/10.1097/00005768-199910000-00013.

Debraux, P., F. Grappe, A. V. Manolova, and W. Bertucci. 2011. "Aerodynamic drag in cycling: Methods of assessment." *Sports Biomech.* 10 (3): 197–218. https://doi.org/10.1080/14763141.2011.592209.

Defraeye, T., B. Blocken, E. Koninckx, P. Hespel, and J. Carmeliet. 2011. "Computational fluid dynamics analysis of drag and convective heat transfer of individual body segments for different cyclist positions." *J. Biomech.* 44 (9): 1695–1701. https://doi.org/10.1016/j.jbiomech.2011.03.035.

de Groot, G., A. J. Sargeant, and J. Geysel. 1995. "Air friction and rolling resistance during cycling." *Med. Sci. Sports Exercise* 27 (7): 1090–1095. https://doi.org/10.1249/00005768-199507000-00020.

di Prampero, P. E. 1986. "The energy cost of human locomotion on land and in water." *Int. J. Sports Med.* 7 (02): 55–72. https://doi.org/10.1055/s-2008-1025736.

di Prampero, P. E., G. Cortili, P. Mognoni, and F. Saibene. 1979. "Equation of motion of a cyclist." *J. Appl. Physiol.* 47 (1): 201–206. https://doi.org/10.1152/jappl.1979.47.1.201.

Faria, E. W., D. L. Parker, and I. E. Faria. 2005. "The science of cycling: Factors affecting performance—Part 2." *Sports Med.* 35 (4): 313–337. https://doi.org/10.2165/00007256-200535040-00003.

Fintelman, D. M., H. Hemida, M. Sterling, and F.-X. Li. 2015. "CFD simulations of the flow around a cyclist subjected to crosswinds." *J. Wind Eng. Ind. Aerodyn.* 144: 31–41. https://doi.org/10.1016/j.jweia.2015.05.009.

Fintelman, D. M., M. Sterling, H. Hemida, and F.-X. Li. 2014. "The effect of crosswinds on cyclists: An experimental study." *Procedia Eng.* 72: 720–725. https://doi.org/10.1016/j.proeng.2014.06.122.

Gross, A. C., C. R. Kyle, and D. J. Malewicki. 1983. "The aerodynamics of human-powered land vehicles." *Sci. Am.* 249 (6): 142–152. https://doi.org/10.1038/scientificamerican1283-142.

Heinen, E., B. van Wee, and K. Maat. 2010. "Commuting by bicycle: An overview of the literature." *Transp. Rev.* 30 (1): 59–96. https://doi.org/10.1080/01441640903187001.

Iseki, H., and M. Tingstrom. 2014. "A new approach for bikeshed analysis with consideration of topography, street connectivity, and energy consumption." *Comput. Environ. Urban Syst.* 48 (Nov): 166–177. https://doi.org/10.1016/j.compenvurbsys.2014.07.008.

Isvan, O. 2015. "Wind speed, wind yaw and the aerodynamic drag acting on a bicycle and rider." *J. Sci. Cycling* 4 (1): 42–50.

Knight, R. 2008. "The bicyclist's paradox." *Phys. Teach.* 46 (5): 275–279. https://doi.org/10.1119/1.2909744.

Kyle, C. R., and E. Burke. 1984. "Improving the racing bicycle." *Mech. Eng.* 106 (9): 34–45.

Martin, J. C., C. J. Davidson, and E. R. Pardyjak. 2007. "Understanding sprint-cycling performance: The integration of muscle power, resistance, and modeling." *Int. J. Sports Physiol. Perform.* 2 (1): 5–21. https://doi.org/10.1123/ijspp.2.1.5.

Martin, J. C., D. L. Milliken, J. E. Cobb, K. L. McFadden, and A. R. Coggan. 1998. "Validation of a mathematical model for road cycling power." *J. Appl. Biomech.* 14 (3): 276–291. https://doi.org/10.1123/jab.14.3.276.

Mercat, N. 1999. "Modelling of bicycle journeys: Using energy expended rather than journey time or distance." In *Proc., 11th Int. Bicycle Planning Conf.* Brussels, Belgium: European Cyclists' Federation.

Mueller, N., D. Rojas-Rueda, T. Cole-Hunter, A. de Nazelle, E. Dons, R. Gerike, T. Götschi, L. Int Panis, S. Kahlmeier, and M. Nieuwenhuijsen 2015. "Health impact assessment of active transportation: A systematic review." *Preventive Med.* 76: 103–114. https://doi.org/10.1016/j.ypmed.2015.04.010.

Navin, F. P. D. 1994. "Bicycle traffic flow characteristics: Experimental results and comparisons." *ITE J.* 64 (3): 31–37.

Olds, T. S. 2001. "Modelling human locomotion: Applications to cycling." *Sports Med.* 31 (7): 497–509. https://doi.org/10.2165/00007256-200131070-00005.

Parkin, J., and J. Rotheram. 2010. "Design speeds and acceleration characteristics of bicycle traffic for use in planning, design and appraisal." *Transp. Policy* 17 (5): 335–341. https://doi.org/10.1016/j.tranpol.2010.03.001.

Preda, I. C., and D. Ciolan. 2010. "Coast-down test—Theoretical and experimental approach." In *The Automobile and the Environment*, 277–288. Brasov, Romania: Transilvania University Press.

Scrucca, L. 2013. "GA: A package for genetic algorithms in R." *J. Stat. Software* 53 (4): 1–37. https://doi.org/10.18637/jss.v053.i04.

Twaddle, H., T. Schendzielorz, and O. Fakler. 2014. "Bicycles in urban areas." *Transp. Res. Rec.* 2434: 140–146. https://doi.org/10.3141/2434-17.

USEPA. 2010. "MOVES2010 highway vehicle population and activity data." No. EPA-420-R-10-026. Washington, DC: USEPA.

Waltham, C., and B. Copeland. 1999. "Power requirements for rollerblading and bicycling." *Phys. Teacher* 37 (6): 379–382. https://doi.org/10.1119/1.880355.

White, R. A., and H. H. Korst. 1972. "The determination of vehicle drag contributions from coast-down tests." In *SAE Technical Paper 720099*. Warrendale, PA: Society of Automotive Engineers.

Wilson, D. G. 2004. *Bicycling science*. 3rd ed. Cambridge, MA: MIT Press.